J Math Chem (2014) 52:575–587
DOI 10.1007/s10910-013-0278-9

ORIGINAL PAPER

Application of the log-normal model for long term high affinity antibody/antigen interactions using Bio-Layer Interferometry

Jakob Wallner · Manfred Kühleitner · Norbert Brunner · Gabriele Lhota · Karola Vorauer-Uhl

Received: 29 April 2013 / Accepted: 3 July 2013 / Published online: 6 December 2013

Abstract For more than 50 years, optical biosensors have been used to measure biomolecular interactions. The most frequently applied binding model to fit biosensor data is the simple 1:1 binding model which requires the stabilization of the association phase to the equilibrium *Req* and the stabilization of the dissociation phase to the equilibrium zero. However, due to technical limitations many published biosensor measurements are finished before these requirements are fulfilled. In the present study, a long term binding interaction analysis with a monoclonal antibody, namely IgG 2F5 and UG37 a specific antigen with a promising biosensor platform, the Bio-Layer Interferometry, was performed. Data fitting with the simple 1:1 binding model to the association phase was inappropriate and the fitted parameters varied with the concentration and time, which contradicts the theory of the simple 1:1 binding model. Furthermore, extrapolation of the fits with individual times spans compared to 100 % of the obtained data systematically underestimated the actual observed binding curve. Interestingly, an alternative model based on the cumulative distribution function of the log-normal probability distribution remedied the aforementioned problems allowing K_L (which is the analog to the affinity constant K_D) to be estimated. We further demonstrate that this model fits the biosensor data far better and is essentially less affected by the stabilization of the association phase to the equilibrium (*Req*) and the stabilization of the dissociation phase to the equilibrium zero. Finally, extrapolation with the log-normal model predicts the actually observed binding curve in a proper manner.

J. Wallner (✉) · G. Lhota · K. Vorauer-Uhl
Department of Biotechnology, University of Natural Resources and Life Sciences, Muthgasse 11, 1190 Vienna, Austria
e-mail: Jakob.Wallner@boku.ac.at

M. Kühleitner · N. Brunner
Department of Integrative Biology, Institute of Mathematics, University of Natural Resources and Life Sciences, Gregor-Mendel-Straße 33, 1180 Vienna, Austria

Keywords Log-normal model · Simple 1:1 interaction model · Biosensor · Bio-Layer Interferometry · Curve fitting · Antibody/antigen interactions

1 Introduction

Bio-molecular interactions measured with label free optical biosensors have been established for a wide range of applications, in particular for quality control and in process development, thus accurate analytical models for data interpretation are needed [1–3]. However, data interpretation itself is one of the most challenging issues for deriving reliable results [4]. Routinely, biosensor technologies imply full kinetic measurements; including estimation of the association rate (k_a), the dissociation rate (k_d), the binding affinity (K_D), the maximum response (R_{max}) and the response at equilibrium (R_{eq}), determined from a fit of the binding data [5]. The time-dependent binding kinetics are related to specific associations and dissociations, whereas, the association rate constant describes how fast molecules bind and the dissociation rate constant describes how fast complexes fall apart. In detail, kinetics determine whether a certain complex is formed and/or dissociates within a given time span. In contrast, the time independent affinity constant is a parameter for the strength of a complex, which is termed the binding strength. Therefore, the affinity determines how much complex is formed at equilibrium. Eventually, R_{max} is the maximum response and R_{eq} is the calculated response at equilibrium that is determined from a fit of the binding data [6]. In general, a particular binding model has to be used for the correct calculation of biosensor data to obtain the fitted parameters including the rate and affinity constants, R_{max} and R_{eq}. In the vast majority of cases, biosensor data are fitted to a simple 1:1 binding model in which calculations of the fitted parameters are based on the concept that association reaches an equilibrium followed by a complete dissociation [7]. However, it has been repeatedly shown that an extended period of association time would be required to reach equilibrium [8]. The most commonly applied biosensor techniques are Surface Plasmon Resonance (SPR) and Bio-Layer Interferometry (BLI) [9]. A considerable disadvantage using SPR is the fact that in standard SPR the association phase is limited by approximately 100 s (about 150 µL sample volume with a flow rate of 100 µL/min) due to technical reasons [10]. Hence, longer measurements can only be performed with additional equipment as it is assumed that the simple 1:1 interaction model accurately fits both short and long term association phase although equilibrium is obviously not reached. Thus, studies of long term measurements are demanded to approve the accuracy of the simple 1:1 model. Therefore, we measured the well studied high-affinity interaction between a monoclonal antibody (IgG 2F5) immobilized on a disposable optical fibre streptavidin biosensor tip surface via a biotin–streptavidin reaction followed by interactions with the specific antigen (UG37) [11]. After attachment of the antigen UG37 to the b-IgG2F5 coated surface, the thickness of the layer on the surface increased. This increase could be measured since BLI directly correlates the spectral shift ($\Delta\lambda$) with the change in thickness (nm) of the biological layer on the streptavidin (SA) biosensor tips. Thus, a change in optical mass thickness of 1 nm results in a 1 nm shift in the interferometry wave pattern [12]. According to this principle, association was detected by a positive shift caused by the

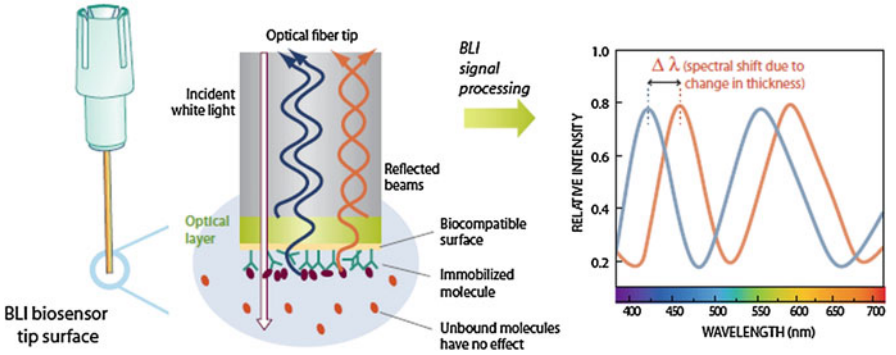

Fig. 1 Principle of the ForteBio BLI technique: *on the left side* a single biosensor-tip is shown followed by a detailed illustration of the analytical technique that analyzes the interference pattern of white light reflected from two biosensor tip surfaces: a layer of immobilized molecules on the biosensor tip, and an internal reference layer. Any change in the number of molecules bound to the biosensor tip causes a shift in the interference pattern that can be measured in real-time. The wavelength shift ($\Delta\lambda$) is a direct measure of the change in thickness of the biological layer as shown *on the right side*. Unbound molecules and changes in the refractive index of the surrounding medium do not affect the interference pattern. (Cited with permission from ForteBio Inc., Menlo Park, CA, USA)

increase in thickness of the layer while dissociation correlated with a negative shift thus providing the basics for data fitting (Fig. 1). Finally, long term binding interaction measurements with an association phase up to at least 8,000 s were performed.

However, to our knowledge, analysis of binding data with the cumulative distribution function of the log-normal probability distribution have not yet been published and thus, our results demonstrate for the first time the suitability of the log-normal model as an appropriate data fitting tool for binding interaction studies. Therefore, the log-normal model was evaluated as an alternative to the simple 1:1 interaction model. The fitting parameters of both models with different time spans and concentrations were compared. Additionally, different initial time spans of the fits from both models were used to compare the extrapolation of the fits.

2 Materials and methods

2.1 Biotinylation of the Antibody (b-IgG2F5) and antigen preparation

Recombinant human monoclonal antibody (IgG2F5) to HIV-1 gp41 epitope ELDKWA and recombinant gp140, envelope protein HIV-1 from the HIV clade A strain 92/UG/037, accession number AY494974, terminating after 2F5 epitope (UG37) was provided by Polymun Scientific GmbH (Klosterneuburg, Austria). Biotinylation of IgG2F5 was performed with NHS-LC-LC-BIOTIN (Pierce, Rockford, USA) according to the manufacturer's protocol. Briefly, IgG2F5 (1,000 μg/ml) in phosphate buffered saline (PBS) was incubated with NHS-LC-LC-BIOTIN in the dark at room temperature for at least 1 h. Finally, unbound biotin was removed using a PD-10 desalting column (GE Healthcare, Vienna, Austria).

2.2 BLI

Octet QK (ForteBio, Menlo Park, CA, USA) was used for BLI studies. Assay was performed in black 96 well plates (Nunc F96 MicroWell™ Plates, Thermo Fisher Scientific, Langenselbold, Germany). The total working volume for samples or buffer was 0.21 ml per well and the rpm setting for each equilibrium, loading, association and dissociation step was 1,000 rpm. The test was performed at 25 °C. Prior to each assay, streptavidin (SA) biosensor tips (ForteBio) were pre-wetted in 0.21 ml PBS for at least 10 min followed by equilibration with PBS for 100 s (s = seconds). Afterwards streptavidin (SA) biosensor tips were non-covalently loaded with b-IgG2F5 in PBS (1:100), followed by an additional equilibration step (100 s). Subsequently, association of b-IgG2F5 with UG37 in a concentration range of c = 1,429, 714.3, 357.1 and 178.6 nM in PBS was conducted. Association at each concentration was carried out for 8,000 s. Finally, the dissociation was monitored with PBS for 1,500 s. All measurements were performed in triplicates.

2.3 Simple 1:1 interaction model

The simple 1:1 interaction model as shown in Fig. 2 is described by the following two formulas [13]:

$$R_t = \frac{k_{on}.c.R_{\max}}{k_{on}.c + k_{off}} \cdot \left(1 - e^{-(k_{on}.c+k_{off}).t}\right), t \leq t_0 \tag{1}$$

for the association phase, and

$$R_t = R_{t_0} \cdot e^{-k_{off}\cdot(t-t_0)}, t \geq t_0 \tag{2}$$

for the dissociation phase

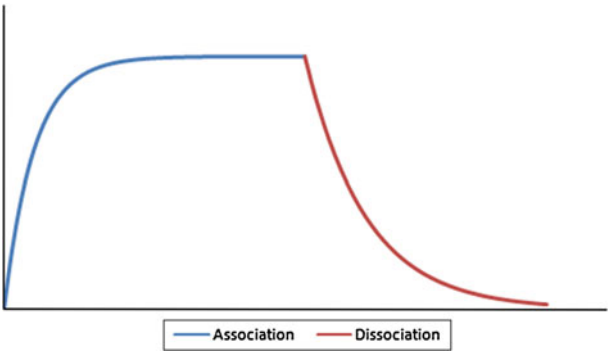

Fig. 2 Association and dissociation phase of the simple 1:1 interaction model which describes the stabilization of the association phase to the equilibrium *Req* and the stabilization of the dissociation phase to the equilibrium zero of a 1:1 interaction, where one ligand molecule interacts with one analyte molecule

The terms have the following meaning:
R_t = biosensor response (signal) at time t
R_{max} = maximal concentration-independent response
k_{off} = concentration-independent dissociation rate (s^{-1})
k_{on} = concentration-independent association constant ($M^{-1}s^{-1}$)
c = concentration in the solution (M)
R_{t0} = initial response for dissociation

The concentration-dependent equilibrium R_{eq} and the time independent affinity constant $K_D(M)$ are described by

$$R_{\mathrm{eq}} = \frac{k_{on}.c.R_{\max}}{k_{on}.c + k_{off}} = R_{\max} \cdot \frac{c.K_D}{1 + c.K_D} \tag{3}$$

$$K_D = k_{on}/k_{off} \tag{4}$$

The kinetic parameters of the simple 1:1 interaction model were determined by a global fit to the biosensor responses.

2.4 Log-normal model

As mentioned above, we compare the simple 1:1 interaction model with an alternative model based on the cumulative distribution function of the log-normal probability distribution [14]:

$$R_t = R_{\max} \cdot (1 - e^{-c.K_L}) \cdot L(t; \mu; \sigma) \tag{5}$$

Here L denotes the lognormal distribution function defined as

$$L(t; \mu; \sigma) = \int_{-\infty}^{t} \frac{1}{\sqrt{2\pi\sigma}} \exp\left(-\frac{(\ln \chi - \mu)^2}{2\sigma^2}\right) d\chi \tag{6}$$

Thereby, R_{max} and μ, σ are constants and these terms have the following meaning:

R_t = biosensor response (signal) at time t
R_{max} = maximal concentration-independent response
$R_{eq} = R_{\max} \cdot (1 - e^{-c.K_L})$ = concentration-dependent equilibrium
c = concentration in the solution (M)
K_L = analogy to K_D (M^{-1})
μ = shape parameter
σ = shape parameter

Hereby, R_{eq} and R_{max} have the same meaning as in the simple 1:1 interaction model. As well as in the simple 1:1 interaction model, the parameters were determined by the least square method.

2.5 Data fitting, fitted parameters and extrapolation of the fits

Most biosensor measurements terminate before stabilization of the association phase to *Req* and the stabilization of the dissociation phase to equilibrium zero. However, kinetic and affinity constants are calculated from this data. Therefore, we fitted 10 % (800 s) and 30 % (2,400 s) of the data and compared these fits to 100 % (8,000 s) of the association data with the *Simple 1:1 interaction model* and the *log-normal model* at different concentrations and scrutinized the effect of the different fits on the fitted parameters. Extrapolation of the fits was performed for illustrative purpose only to explain a typical behavior of the models with respect to the considered data.

The fitted parameters of the initial 10 and 30 % of the data from both models were used to compare different series of the extrapolation of the fits.

Data fitting and *extrapolation of the fits* were performed with Excel spreadsheets (Version 2003, Microsoft, Redmond, WA, USA). The individual fit at each concentration to obtain the fitted parameters were calculated as an average of three independent measurements.

3 Results

3.1 BLI

Long term association experiments using the well established interaction of IgG2F5/UG37 based on the BLI platform were performed to evaluate the quality of the simple 1:1 interaction model in comparison to the log normal concept. Therefore, SA equilibrated biosensor tips were loaded with the b-IgG2F5, retaining a constant loading baseline, resulting in a final capture signal between 2.8 and 3.1 nm within at least 100 s (Fig. 3). These SA biosensor tips were incubated with the specific antigen (UG37) at different concentrations as described in the materials and methods section to measure the corresponding association and dissociation profiles. The quality of the test performance was evaluated carefully to avoid nonspecific interaction of the UG37 antigen with uncoated sensor tips meaning that the streptavidin itself showed no cross reactivity with the analyte (data not shown). In general, the biotin–streptavidin bond is known as one of the strongest non-covalent biological interactions and forms very rapidly, stable complexes in a wide range of pH and temperatures [15].

The interaction of the antigen with the antibody attached on the sensor tips showed concentration dependent association curves as expected. Furthermore, if the antibodies were attached once, no dissociation occurred under native conditions. This indicates that very stable complexes were formed. This phenomenon is not really new and has been observed repeatedly [16].

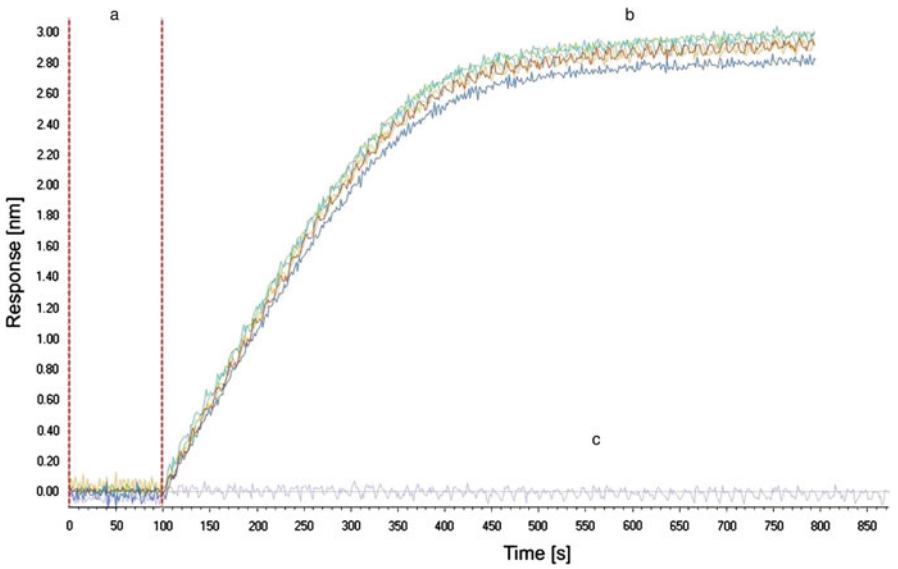

Fig. 3 Typical loading and equilibration curves showing the equilibration step (100 s) with PBS (**a**), the loading step with b-IgG2F5 (**b**) and the reference curve equilibrated and loaded with PBS (**c**), Simultaneous measurements of five individual sensor tips

3.2 Data fitting, fitted parameters and extrapolation of the fits

In Table 1 the fitted parameters of the simple 1:1 interaction model at the individual time spans (800, 2,400 and 8,000 s) and at different concentrations (c = 1,429, 714.3, 357.1 and 178.6 nM) are summarized. The evaluation of kinetic parameters was done by fitting corresponding data according to the simple 1:1 interaction model at different time windows for the same data set. The association rate constant (k_a) is defined as the rate of complex formation per second in a 1 molar solution of two reaction partners, while the dissociation rate constant (k_d) indicates the stability of this complex. The affinity constant K_D is calculated by the ratio of k_d/k_a. As shown, the k_a value with the highest concentration at 800 s is more than three times larger than at 8,000 s and two times larger than at 2,400 s, whereby this discrepancy is larger the higher the concentration. The relative standard deviation (RSD) of the dissociation rate constant (k_d) was 17.7 %, while the RSD was defined as the standard deviation divided by the mean and multiplied by 100 %. The K_D values vary from 0.81×10^{-8} M to 5.91×10^{-8} M depending on concentration and the defined association time. Additionally, the maximum response (R_{max}) and the response at equilibrium (R_{eq}) determined from the fit of the binding data are shown. Furthermore, the fitted parameters of the log-normal model at the individual time spans and at different concentrations are summarized in Table 2. The parameters μ and σ are mere shape parameters that define the geometry of the fitted curve. As shown the RSD of μ and σ is about 11 % whereby these parameters increase with the shorter the time span. The parameter K_L is analogous to K_D and was estimated with $4.52 \times 10^6 M^{-1}$ independent of the concentration and

Table 1 Fitted parameters of the simple 1:1 interaction model

Concentration	1,429 nM			714 nM			357 nM			179 nM		
Time (s)	800	2,400	8,000	800	2,400	8,000	800	2,400	8,000	800	2,400	8,000
k_a ($M^{-1}s^{-1}$)	2,502	1,363	729	2,713	1,693	887	3,791	2,372	1,267	1,721	1,162	1,299
k_d (s^{-1}) $\times 10^{-5}$	4.31			3.24			3.09			3.01		
K_D (M) $\times 10^{-8}$	1.72	3.16	5.91	1.20	1.92	3.65	0.81	1.30	2.44	1.75	2.59	2.32
R_{max}	0.99	1.29	1.59	0.81	1.05	1.38	0.62	0.84	1.15	0.69	0.99	0.88
R_{eq}	0.98	1.26	1.52	0.79	1.02	1.31	0.60	0.81	1.08	0.63	0.87	0.78

Kinetic rate constants, affinity constants, R_{max} and R_{eq} values determined by a global fit to the biosensor data with the simple 1:1 interaction model for the IgG2F5/UG37 interaction with 800 s (10 % of the data), 2,400 s (30 % of the data) and 8,000s (100 % of the data) and at different concentrations (c = 1,429, 714.3, 357.1 and 178.6 nM). All parameters represent the mean values of triplicate measurements of each concentration

the defined association time. It is important to note that the R_{max} and R_{eq} determined with the log-normal model are rather different from the estimated R_{max} and R_{eq} with the simple 1:1 interaction model. In general, the log-normal model fits the binding curve independent of the association time and concentration in a proper manner. The only exception depicts the concentration $c = 178.6$ nM using 10 % of data. In this case the data fit results in a clearly visible deviation (Tab. 2). The fitted parameters from Tables 1 and 2 were used for Figs. 4 and 5 to compare the extrapolations of the fits at different time spans and at different concentrations with both models. The corresponding fits with full set of data (8,000 s) and extrapolation of the fits to predict the remaining 90 and 70 % of the association curve are shown in Figs. 4 and 5. These results demonstrate that the simple 1:1 interaction model at different concentrations is obviously inappropriate to predict the observed binding curve, while the log-normal model describes the individual situation more accurately. The log-normal model provides an excellent fit with full set of data as well as an excellent extrapolation of the fits which predict the actual observed binding curve. In detail, using 10 and 30 % of the association time for the extrapolation, the simple 1:1 interaction model (Fig. 4), at the concentrations c = 1,429, 714.3 and 357.1 nM obviously underestimates the actual observed binding curve.

In contrast, only for the lowest concentration $c = 178.6$ nM and using 10 and 30 % of the data for the extrapolation of the fits, the simple 1:1 interaction model is better than the log-normal model.

4 Discussion

The present study is focused on a comparison of the established simple 1:1 interaction model with an alternative model, based on the cumulative distribution function of the log- normal model. For this approach a long term association phase based on a well established antibody/antigen interaction, namely IgG2F5/UG37 was used [17,18]. All measurements were performed with BLI, a promising biosensor platform, developed by ForteBio with the main focus being to qualify and quantify protein/protein inter-

Table 2 Fitted parameters of the log-normal model

Concentration	1,429 nM			714 nM			357 nM			179 nM		
Time (s)	800	2,400	8,000	800	2,400	8,000	800	2,400	8,000	800	2,400	8,000
μ	7.41	6.65	6.64	7.23	7.34	7.49	8.87	8.39	8.08	6.79	7.58	8.60
σ	2.58	2.22	2.21	1.95	2.01	2.10	2.35	2.19	2.04	0.94	1.24	1.69
K_L (1/M) $\times 10^6$	4.52	4.52	4.52	4.52	4.52	4.52	4.52	4.52	4.52	4.52	4.52	4.52
R_{max}	2.12	1.88	1.95	2.12	1.88	1.95	2.12	1.88	1.95	2.12	1.88	1.95
R_{eq}	2.49	1.9	1.89	1.63	1.71	1.81	2.31	1.86	1.65	0.34	0.65	1.18

Shape parameters (μ, σ), K_L (which is the analog to the affinity constant K_D), R_{max} and R_{eq} values determined by fitting with the log-normal model for the IgG2F5/UG37 interaction with 800 s (10 % of the data), 2,400 s (30 % of the data) and 8,000 s (100 % of the data) and at different concentrations ($c = 1{,}429$, 714.3, 357.1 and 178.6 nM). All parameters represent the mean values of triplicate measurements of each concentration

actions in research and routine applications [19]. In this study, we could illustrate that data interpretation is still a major topic and therefore the specific rate and affinity constants calculated from the simple 1:1 interaction model should be interpreted with caution for various reasons. This is especially in the case of slow kinetics (with respect to association and dissociation). It should be noted that *Req* and the stabilization of the dissociation phase to the equilibrium zero (which are the prerequisites for the calculation of kinetic rate constants) need to be estimated properly. Figure 2 shows the association and dissociation phases in an ideal situation for the simple 1:1 interaction model where both the stabilization of the association phase to R_{eq} can be observed, with the stabilization of the dissociation phase to the equilibrium zero also observable assuming complete binding reversibility. However, in many biosensor experiments the association phase is terminated before the equilibrium has been reached, mainly due to technical reasons [8]. In contrast, the used BLI technology the opportunity to prolong the association phase without any technical modifications [20]. In this study an association phase of 8,000 s was used. In common SPR experiments the association phase is approximately 100fold smaller than in our experiments [21]. The main objectives of this study were to compare curve fitting and the calculated parameters with the simple 1:1 interaction model and the log-normal model. Furthermore, the influence of the selected association time on the fitted parameters and extrapolation of the fits, to predict the binding curve, were compared. We could demonstrate that the 1:1 model has distinct weaknesses:

1. Data fitting to the association phase was inappropriate (Table 1; Fig. 4.);
2. The kinetic constants varied with concentration and time (Table 1);
3. Extrapolations of the fits were underestimated the actual observed binding curve (Fig. 4.)

In summary, especially for slow high affinity binding interactions and long term measurements, the simple 1:1 interaction model may not be the best option. A more detailed consideration explains this phenomenon: R_{eq} and R_{max} are essentially dependent on the duration of the measurements. Consequently, the shorter the duration of the measurements the lower was the computed R_{eq}, R_{max}, K_D and the higher k_a. Finally,

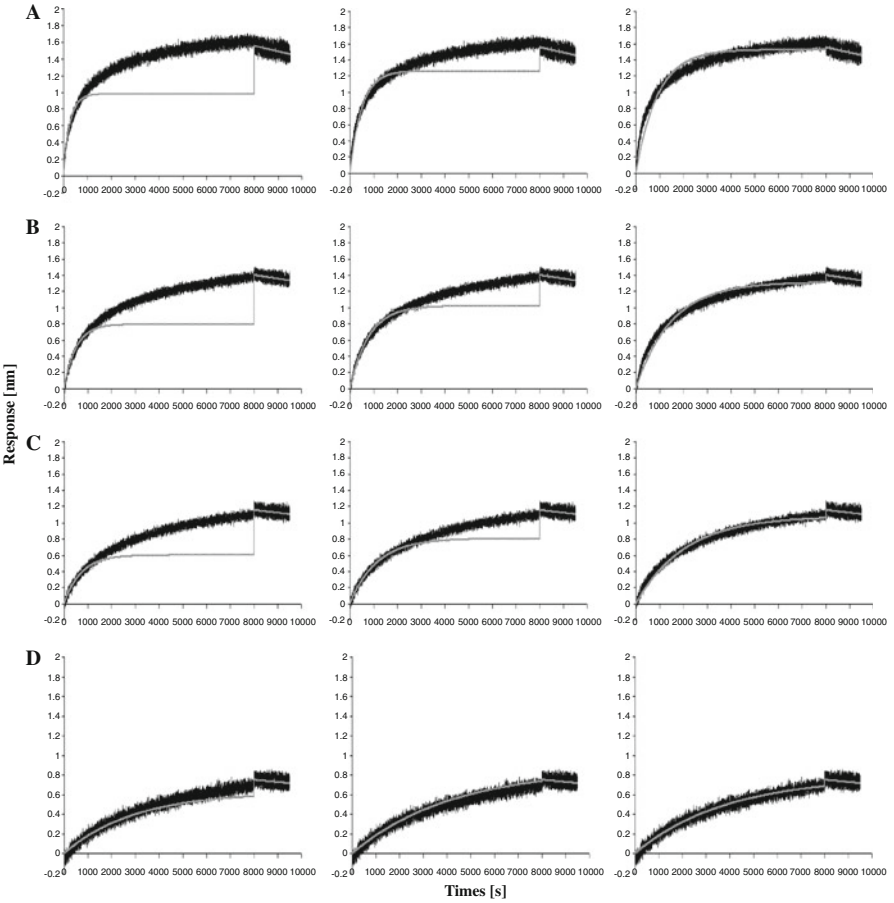

Fig. 4 Data fitting and extrapolations of the fits with the simple 1:1 interaction model for an extended association (0–8,000 s) and dissociation (8,000–9,500 s) phase for the IgG2F5/UG37 interaction: The *black traces* represent the experimental data and the *grey traces* represent the fits with the 1:1 binding model. Extrapolations of fits at 10 % of the data (800 s; *fitted curves* at the *left side*) 30 % of the data (2,400 s; *fitted curves* in the *middle*) and 100 % of the data (8,000 s; *fitted curves* at the *left side*) are shown. The individual antigen concentrations were 1,428.5 nM (**a**), 714.3 nM (**b**), 357.1 nM (**c**) and 178.6 nM (**d**). *All curves* represent the mean values of triplicate measurements of each concentration

the rate and affinity constants varied, depending on the concentration and duration of measurement. These obtained results are in contradiction to the definition of the simple 1:1 interaction model [22]. Due to this circumstance, correct calculation of the rate and affinity constants with the simple 1:1 interaction model could fail and thus, the authors considered an alternative model. The cumulative distribution function of the log-normal probability distribution (as an alternative model) substantially improves the quality of the data fits. Misfits observed with the 1:1 model were significantly reduced, the calculated parameters were seen to be quite stable (Table 2) and extrapolations of the fits predict the observed binding curves quite well. In conclusion, the log-normal function seems to be more convenient for fitting interactions which deviate

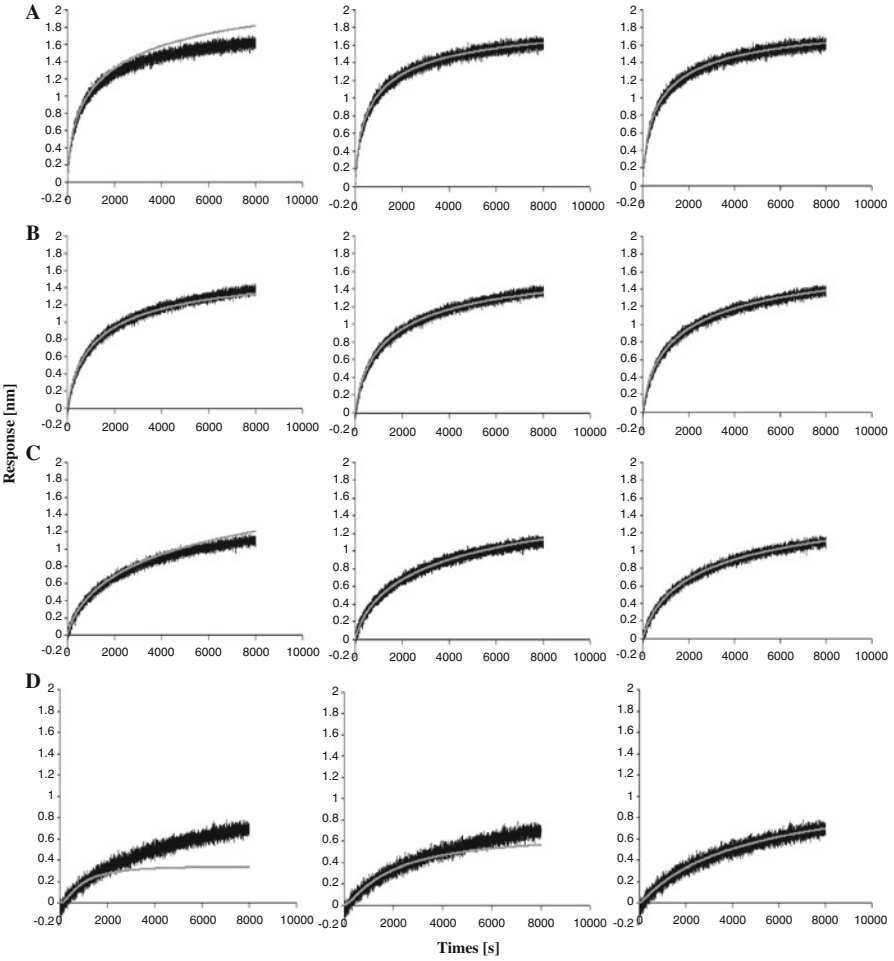

Fig. 5 Data fitting and extrapolations of the fits with the log-normal model for an extended association phase (0–8,000 s) for the IgG2F5/UG37 interaction: The *black traces* represent the experimental data and the *grey traces* represent the fits with log-normal model. Extrapolations of fits at 10 % of the data (800 s; *fitted curves* at the *left side*) 30 % of the data (2,400 s; *fitted curves* in the *middle*) and 100 % of the data (8,000 s; *fitted curves* at the *left side*) are shown. The individual antigen concentrations were 1,428.5 nM (**a**), 714.3 nM (**b**), 357.1 nM (**c**) and 178.6 nM (**d**). *All curves* represent the mean values of triplicate measurements of each concentration

from an optimal binding situation, independent of the selected association time, the concentration of the analyte and the dissociation process.

Although the fit of the log-normal model describes the response that is directly observable in a more appropriate way, it is not able to provide information about the rate constants. However, R_{eq} and $R_{\max}$ have the same meaning in both models and K_L is an analog to K_D. Finally, it should be reemphasized that many bio-molecular interactions will adhere in the simple 1:1 interaction model. However, in this study we demonstrate that the fitted parameters with the simple 1:1 interaction model can be affected by the selected association time span and therefore, published kinetic

constants should be scrutinised critically, particularly when curve fitting is not shown and/or equilibrium is not reached. The question therefore is whether a good curve fit and a visual inspection of the binding curve should be a priority instead of still reporting binding constants. Overall, we could demonstrate that the log-normal model provides an excellent curve fitting tool for biomolecular interactions. Thus, the paper presents a new modelling approach to biosensor data and relatively short measurement intervals are needed to estimate reasonably the R_{eq}, R_{max} and K_L values and the extrapolations of the fits properly represent the actual observed binding curves (Fig. 5). Future research will concentrate on the question about estimation of rate constants with the log-normal model. From the results presented here, we predict the problems to be most pronounced for high affinity interactions with slow kinetics. These findings have profound implications in all areas related to studying bio-molecular interactions, using biosensor technologies.

Acknowledgments The authors thank Polymun Scientific, Immunbiologische Forschung GmbH (Klosterneuburg, Austria), for kindly providing the recombinant human monoclonal antibody (IgG2F5) and the specific antigen UG37 in pharmaceutical grade.

References

1. A. Giannetti, B. Koch, M. Browner, J. Med. Chem. **51**, 574 (2008)
2. R.L. Rich, G.A. Papalia, P.J. Flynn, J. Furneisen, J. Quinn, J.S. Klein, P.S. Katsamba, M.B. Waddell, M. Scott, J. Thompson, J. Berlier, S. Corry, M. Baltzinger, G. Zeder-Lutz, A. Schoenemann, A. Clabbers, S. Wieckowski, M.M. Murphy, P. Page, T.E. Ryan, J. Duffner, T. Ganguly, J. Corbin, S. Gautam, G. Anderluh, A. Bavdek, D. Reichmann, S.P. Yadav, E. Hommema, E. Pol, A. Drake, S. Klakamp, T. Chapman, D. Kernaghan, K. Miller, J. Schuman, K. Lindquist, K. Herlihy, M.B. Murphy, R. Bohnsack, B. Andrien, P. Brandani, D. Terwey, R. Millican, R.J. Darling, L. Wang, Q. Carter, J. Dotzlaf, J. Lopez-Sagaseta, I. Campbell, P. Torreri, S. Hoos, P. England, Y. Liu, Y. Abdiche, D. Malashock, A. Pinkerton, M. Wong, E. Lafer, C. Hinck, K. Thompson, C.D. Primo, A. Joyce, J. Brooks, F. Torta, A.B. Bagge Hagel, J. Krarup, J. Pass, M. Ferreira, S. Shikov, M. Mikolajczyk, Y. Abe, G. Barbato, A.M. Giannetti, G. Krishnamoorthy, B. Beusink, D. Satpaev, T. Tsang, E. Fang, J. Partridge, S. Brohawn, J. Horn, O. Pritsch, G. Obal, S. Nilapwar, B. Busby, G. Gutierrez-Sanchez, R.D. Gupta, S. Canepa, K. Witte, Z. Nikolovska-Coleska, Y.H. Cho, R. D'Agata, K. Schlick, R. Calvert, E.M. Munoz, M.J. Hernaiz, T. Bravman, M. Dines, M.H. Yang, D.G. Myszka, Anal. Biochem. **386**, 194 (2009)
3. D. Myszka, X. He, M. Dembo, T. Morton, B. Goldstein, Biophys. J. **75**, 583 (1998)
4. S.P. Yadav, S. Bergqvist, M.L. Doyle, T.A. Neubert, A.P. Yamniuk, J. Biomol. Tech. **23**, 94 (2012)
5. A. Onell, K. Andersson, J. Mol. Recognit. **18**, 307 (2005)
6. Y.N. Abdiche, Biosensors **302**, 81 (2010)
7. D.G. Myszka, J. Mol. Recognit. **12**, 279 (1999)
8. D.G. Myszka, M.D. Jonsen, B.J. Graves, Anal. Biochem. **265**, 326 (1998)
9. R. Barbour, M.P. Bova, Bioanalysis **4**, 619 (2012)
10. I. Navratilova, E. Eisenstien, D.G. Myszka, Anal. Biochem. **344**, 295 (2005)
11. B. Ma, M. Alam, E. Go, X. Lu, H. Desaire, G. Tomaras, C. Bowman, L. Sutherland, R. Scearce, S. Santra, N. Letvin, T. Kepler, H. Liao, B. Haynes, Plos Pathogens **7**, 1 (2011)
12. T. Do, F. Ho, B. Heidecker, K. Witte, L. Chang, L. Lerner, Protein Expr. Purif. **60**, 150 (2008)
13. D.J. O'Shannessy, M. Brigham-Burke, K.K. Soneson, P. Hensley, I. Brooks, Anal. Biochem. **212**, 457 (1993)
14. J. Tintner, M. Kühleitner, E. Binner, N. Brunner, E. Smidt, Biodegradation **23**, 407 (2012)
15. A. Holmberg, A. Blomstergren, O. Nord, M. Lukacs, J. Lundeberg, M. Uhlen, Electrophoresis **26**, 501 (2005)
16. Y.N. Abdiche, D.G. Myszka, Anal. Biochem. **328**, 233 (2004)
17. J.R. Mascola, M.K. Louder, T.C. VanCott, C.V. Sapan, J.S. Lambert, L.R. Muenz, B. Bunow, D.L. Birx, M.L. Robb, J. Virol. **71**, 7198 (1997)

18. A. Dey, K. David, P. Klasse, J. Moore, Virology **360**, 199 (2007)
19. Y. Abdiche, D. Malashock, A. Pinkerton, J. Pons, Anal. Biochem. **377**, 209 (2008)
20. J. Wallner, G. Lhota, D. Jeschek, A. Mader, K. Vorauer-Uhl, J. Pharm. Biomed. Anal. **72**, 150 (2013)
21. P.S. Katsamba, I. Navratilova, M. Calderon-Cacia, L. Fan, K. Thornton, M. Zhu, T.V. Bos, C. Forte, D. Friend, I. Laird-Offringa, G. Tavares, J. Whatley, E. Shi, A. Widom, K.C. Lindquist, S. Klakamp, A. Drake, D. Bohmann, M. Roell, L. Rose, J. Dorocke, B. Roth, B. Luginbühl, D.G. Myszka, Anal. Biochem. **352**, 208 (2006)
22. D.J. O'Shannessy, M. Brigham-Burke, K.K. Soneson, P. Hensley, I. Brooks, Methods Enzymol. **240**, 323 (1994)